

The stochastic counterpart of conservation laws with heterogeneous conductivity fields: application to deterministic problems and uncertainty quantification

Amir H. Delgoshaie^{a,*}, Peter W. Glynn^b, Patrick Jenny^c, Hamdi A. Tchelepi^a

^a*Department of Energy Resources Engineering, Stanford University. 367 Panama Street, Stanford, CA, 94305, USA*

^b*Department of Management Science and Engineering, Stanford University. 475 Via Ortega, Stanford, CA, 94305, USA*

^c*Institute of Fluid Dynamics, ETH Zürich. Sonneggstrasse 3, CH-8092 Zürich, Switzerland*

Abstract

Conservation laws in the form of elliptic and parabolic partial differential equations (PDEs) are fundamental to the modeling of many applications such as heat transfer and flow in porous media. Based on the relation between stochastic diffusion processes and PDEs, Monte Carlo (MC) methods are available to solve these PDEs in cases where the conductivity field used in the conservation law is homogeneous. In many problems of interest, the conductivity field is highly heterogeneous, and existing stochastic solution strategies are not directly applicable. Here, we describe a MC method to solve conservation laws with heterogeneous conductivity fields using general diffusion processes. In addition to using the conductivity field to describe diffusion, it is shown that the gradient of the conductivity field will play the role of a drift term in the proposed random walks. The stochastic representation of the conservation law makes it possible to compute the solution without a computational mesh. Moreover, the solution at any location can be computed independently of the solution at other locations in the domain. The methodology is demonstrated using problems governed by deterministic and stochastic PDEs. It is shown that the method provides an efficient alternative to compute the statistical moments of the solution to a stochastic PDE at any point in the domain.

Keywords: heterogeneous diffusion, stochastic modeling, backward equations

*Corresponding author

Email addresses: amirdel@stanford.edu (Amir H. Delgoshaie), glynn@stanford.edu (Peter W. Glynn), jenny@ifd.mavt.ethz.ch (Patrick Jenny), tchelepi@stanford.edu (Hamdi A. Tchelepi)

1. Introduction

Elliptic and Parabolic partial differential equations (PDEs) arise in many applications in describing conservation laws. The mass conservation equation resulting from Fick’s law, the heat equation, and the pressure equation in the context of flow in porous media are some of the prominent examples of such applications. These equations have the following general form

$$\nabla \cdot (\mathbf{K} \nabla p) = c \frac{\partial p}{\partial t}, \quad (1)$$

when the problem is time dependent and

$$\nabla \cdot (\mathbf{K} \nabla p) = 0, \quad (2)$$

when the problem is at steady state. Here, p is the unknown (concentration, temperature, or pressure) and \mathbf{K} is the conductivity tensor. In these problems, the flux (of mass or heat) is governed by a Fick’s type law

$$q = \mathbf{K} \nabla p. \quad (3)$$

In many practical settings, closed-form solutions of PDEs 1 and 2 do not exist, and numerical methods such as finite-volume (FV), and finite-element method are used to compute numerical solutions of these PDEs [1]. These numerical methods rely on discretization of the PDE for the domain of interest and deriving a set of linear equations for the solution of the PDE on the discretized grid. Once the system is reduced to a linear system, efficient numerical methods have been developed to solve that system [2]. These linear solvers compute the solution for all grid points simultaneously.

In stochastic modeling, elliptic and parabolic PDEs that are similar to equations 1 and 2 arise when calculating various expected values for a stochastic diffusion process [3]. In the stochastic modeling nomenclature, these PDEs are referred to as backward equations, and the differential operator describing the left-hand-side of equations 1 and 2 is referred to as \mathcal{L} . In the view of the connection between diffusion processes and PDEs, the stochastic counterpart of \mathcal{L} has been used in methods such as backward walks [4] and random walks on boundary [5] to solve equations 1 and 2 for cases where the conductivity field is homogeneous. In many applications, such as flow in natural porous formations, the conductivity field is highly heterogeneous, and this heterogeneity plays an important role in dictating the flow behavior. Here, we show how stochastic representations can be used to model these PDEs with heterogeneous conductivity fields.

Recognizing that equations 1 and 2 correspond to backward equations of specific stochastic processes has multiple advantages. First, unlike solving linear systems, by using the stochastic representation of the problem, the solution

for any subset of points in the domain can be found independently of the solution at points outside the subset of interest. Second, the numerical solution can be computed at any point in the domain without the need for a mesh. Third, the stochastic solution strategy is ‘embarrassingly parallel’, and that allows for efficient implementations that can take full advantage of GPUs and massively parallel CPUs.

These advantages become more important in the case where there is uncertainty in \mathbf{K} and one would need to solve the equations for an ensemble of realizations to compute the statistical moments, or the distribution, of the dependent variable. Using the stochastic strategy, the one-point PDF at any location in the domain is obtained by computing the solution only at the point of interest - independently of others points in the domain - for the different realizations of the conductivity field.

In this paper, we show the correspondence between \mathcal{L} , the operator in the backward equations of diffusion processes, and the differential operator in the steady-state and transient conservation equations with heterogeneous coefficients. In the next section, the stochastic representation of equations 1 and 2 is discussed in detail, and the specific drift and diffusion functions that correspond to heterogeneous conductivity fields are described. In section 3, we discuss two numerical examples that illustrate the proposed stochastic method to solve deterministic problems. In section 4, an example with uncertain \mathbf{K} is considered, and the one-point PDF and the moments of the distributions are estimated using the proposed Monte Carlo method. Conclusions and future work are discussed in section 5.

2. Conservation laws versus backward equations

In the context of stochastic processes, backward equations arise when finding various expected values. Specifically, in the context of stochastic differential equations (SDEs), if $X(t)$ satisfies

$$dX(t) = \mu(X(t))dt + \sigma(X(t))dB(t), \quad (4)$$

then [3]

$$u^*(t, x) = E[r(X(t)) | X(0) = x] = E_x[r(X(t))], \quad (5)$$

which is the expected value of $r(X(t))$ if we start from $X(0) = x$, can be found by solving the following parabolic PDE

$$\begin{aligned} \mathcal{L}u^*(x, t) &= \frac{\partial u^*(x, t)}{\partial t} \\ u^*(x, 0) &= r(x), \end{aligned} \quad (6)$$

where the differential operator \mathcal{L} is defined as follows

$$\mathcal{L} = \sum_{i=1}^d \mu_i(x) \frac{\partial}{\partial x_i} + \frac{1}{2} \sum_{i,j=1}^d b_{ij}(x) \frac{\partial^2}{\partial x_i \partial x_j}. \quad (7)$$

Here

$$b_{ij}(x) = \sigma(x) \sigma(x)^T. \quad (8)$$

In these equations, $X(t), \mu(X(t)) \in \mathbb{R}^d$ and $\sigma(X(t)) \in \mathbb{R}^{d \times m}$. $B(t) \in \mathbb{R}^d$ is a d -dimensional Brownian motion. For example, in 2D b_{ij} is

$$b_{ij}(x) = \sigma(x) \sigma(x)^T = \begin{bmatrix} \sigma_{11} & \sigma_{12} \\ \sigma_{21} & \sigma_{22} \end{bmatrix} \begin{bmatrix} \sigma_{11} & \sigma_{21} \\ \sigma_{12} & \sigma_{22} \end{bmatrix} = \begin{bmatrix} \sigma_{11}^2 + \sigma_{12}^2 & \sigma_{11}\sigma_{21} + \sigma_{12}\sigma_{22} \\ \sigma_{11}\sigma_{21} + \sigma_{12}\sigma_{22} & \sigma_{21}^2 + \sigma_{22}^2 \end{bmatrix}. \quad (9)$$

The connection between equations 4 and 6 makes it possible to solve a PDE similar to equation 6 using MC simulation of its SDE counterpart. The algorithm is as follows: to find $u^*(x, t)$, launch random walks from x at time t ; evolve them according to equation 4 for t time units backward in time (to $t = 0$), and store $r(X(0))$. The solution is then the average of the stored values $r(X(0))$. For homogeneous conductivity fields ($\mathbf{K}_{ij} = K$), this method is referred to as ‘backward walks’ [4].

Similarly, the expected value

$$u^*(x) = E_x[r(X(T))], \quad (10)$$

where $T = \inf\{t \geq 0 : X(t) \in C^c\}$ is the first hitting time of C^c (complement of set C), can be found by solving the following elliptic PDE

$$\begin{aligned} \mathcal{L}u^*(x) &= 0, \quad x \in C \\ u^*(x) &= r(x), \quad x \in C^c. \end{aligned} \quad (11)$$

Hence, to solve a PDE similar to equation 11, one can use MC simulations of equation 4. The algorithm is as follows: to find $u^*(x)$, start many random walks from x , and evolve them according to equation 4 until they hit the boundary for the first time, then store the boundary value at the hitting times. The solution can be obtained by averaging these boundary values. For cases where the conductivity field is homogeneous, this method has been developed and is referred to as random walk on boundary [5].

In order to use backward walks and random walks on boundary for problems where the conductivity field is heterogeneous, we need to find the stochastic counterpart of the differential operator in equations 1 and 2. In the following section, we find this stochastic representation by expanding the conservation equations and comparing the expanded operator with \mathcal{L} . Two different cases

are considered, the case where the off-diagonal terms of the conductivity tensor are zero and the case where they are non-zero. For both cases, the comparison is performed for a two-dimensional system; however, the argument can readily be extended to n dimensions.

2.1. Zero off-diagonals, $K_{12} = K_{21} = 0$

Since the linear operator for both elliptic and parabolic problems is the same, we focus on the elliptic problem. Expansion of equation 2 leads to

$$\nabla \cdot (K_{11} \frac{\partial p}{\partial x_1} e_1 + K_{22} \frac{\partial p}{\partial x_2} e_2) = 0, \quad (12)$$

$$\frac{\partial K_{11}}{\partial x_1} \frac{\partial p}{\partial x_1} + \frac{\partial K_{22}}{\partial x_2} \frac{\partial p}{\partial x_2} + K_{11} \frac{\partial^2 p}{\partial x_1^2} + K_{22} \frac{\partial^2 p}{\partial x_2^2} = 0. \quad (13)$$

Equation 13 can be written as $\mathcal{L}_1 p = 0$, where

$$\mathcal{L}_1 = \left(\frac{\partial K_{11}}{\partial x_1} \frac{\partial}{\partial x_1} + \frac{\partial K_{22}}{\partial x_2} \frac{\partial}{\partial x_2} \right) + \left(K_{11} \frac{\partial^2}{\partial x_1^2} + K_{22} \frac{\partial^2}{\partial x_2^2} \right). \quad (14)$$

The first part of \mathcal{L}_1 matches the drift term of the backward operator. Note that the derivatives of the conductivity field constitute the drift term, or the preferential direction for the random walks. In two dimensions, comparison of b_{ij} and the second-order term in \mathcal{L}_1 yields

$$\begin{bmatrix} K_{11} & 0 \\ 0 & K_{22} \end{bmatrix} = \frac{1}{2} \begin{bmatrix} \sigma_{11}^2 + \sigma_{12}^2 & \sigma_{11}\sigma_{21} + \sigma_{12}\sigma_{22} \\ \sigma_{11}\sigma_{21} + \sigma_{12}\sigma_{22} & \sigma_{22}^2 + \sigma_{21}^2 \end{bmatrix}. \quad (15)$$

Choosing $\sigma_{11} = \sqrt{2K_{11}}$ and $\sigma_{22} = \sqrt{2K_{22}}$, and $\sigma_{12} = \sigma_{21} = 0$ will satisfy system 15. These are the diffusion coefficient used in random walk on boundary and backward walks for homogeneous conductivity fields.

2.2. Non-zero off-diagonals, $K_{12} = K_{21} \neq 0$

Similar to the previous section, we expand equation 2 and obtain

$$\nabla \cdot (K_{11} \frac{\partial p}{\partial x_1} e_1 + K_{22} \frac{\partial p}{\partial x_2} e_2 + K_{12} \frac{\partial p}{\partial x_2} e_1 + K_{21} \frac{\partial p}{\partial x_1} e_2) = 0, \quad (16)$$

$$\begin{aligned} & \frac{\partial K_{11}}{\partial x_1} \frac{\partial p}{\partial x_1} + \frac{\partial K_{22}}{\partial x_2} \frac{\partial p}{\partial x_2} + \frac{\partial K_{12}}{\partial x_1} \frac{\partial p}{\partial x_2} + \frac{\partial K_{21}}{\partial x_2} \frac{\partial p}{\partial x_1} + \\ & K_{11} \frac{\partial^2 p}{\partial x_1^2} + K_{22} \frac{\partial^2 p}{\partial x_2^2} + K_{12} \frac{\partial^2 p}{\partial x_1 \partial x_2} + K_{21} \frac{\partial^2 p}{\partial x_2 \partial x_1} = 0 \end{aligned} \quad (17)$$

Equation 17 can be written as $\mathcal{L}_2 p = 0$, where

$$\begin{aligned} \mathcal{L}_2 = & \left(\left(\frac{\partial K_{11}}{\partial x_1} + \frac{\partial K_{21}}{\partial x_2} \right) \frac{\partial}{\partial x_1} + \left(\frac{\partial K_{22}}{\partial x_2} + \frac{\partial K_{12}}{\partial x_1} \right) \frac{\partial}{\partial x_2} \right) + \\ & \left(K_{11} \frac{\partial^2}{\partial x_1^2} + K_{22} \frac{\partial^2}{\partial x_2^2} + K_{12} \frac{\partial^2}{\partial x_1 \partial x_2} + K_{21} \frac{\partial^2}{\partial x_2 \partial x_1} \right) \end{aligned} \quad (18)$$

The first-order part of \mathcal{L}_2 matches the drift term in the backward operator. Comparison of the second-order terms leads to the following:

$$\begin{bmatrix} K_{11} & K_{12} \\ K_{21} & K_{22} \end{bmatrix} = \frac{1}{2} \begin{bmatrix} \sigma_{11}^2 + \sigma_{12}^2 & \sigma_{11}\sigma_{21} + \sigma_{12}\sigma_{22} \\ \sigma_{11}\sigma_{21} + \sigma_{12}\sigma_{22} & \sigma_{22}^2 + \sigma_{21}^2 \end{bmatrix}. \quad (19)$$

System 19 consists of four equations and four unknowns which can be easily solved to find the σ_{ij} corresponding to L_2 .

3. Illustrative deterministic examples

In the previous section, the stochastic counterpart of the conservation equations 1 and 2 was derived. In this section, two examples of using the proposed stochastic method for solving deterministic problems are provided. In the first example, the conductivity field is known analytically. In the second example, we consider one realization of a Gaussian conductivity field with a given mean and covariance.

3.1. Example 1: $K(x) = x^2$

Here, we consider a one dimensional case, where $K(x) = x^2$. The domain is the line segment between one and two, $D = [1, 2]$, and the boundary conditions are $p(1) = 1$ and $p(2) = 0$. Having a simple closed form conductivity, we can easily calculate the derivative of the conductivity field, $dK/dx = 2x$. Moreover it can be easily verified that $p(x) = 2/x - 1$ is the solution to this elliptic problem.

The Monte Carlo estimate of this solution at various points in the domain are compared to the analytical solution in Fig. 1, for different number of MC trials. The number of trials are the number of random walks that we launch from every point of interest. It can be seen that even for small number of trials, MC provides a good estimate of the solution and the estimate improves by increasing the number of trials.

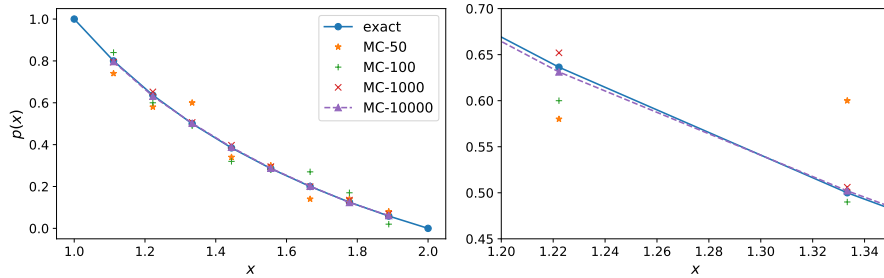


Figure 1: Comparison of the analytic solution with the MC estimates for example 1, for different number of MC trials with $dt = 1e-5$.

3.2. Example 2: one realization of a random field

Here, we consider a one dimensional case, where $K(x)$ has a log-normal distribution with mean zero and variance one ($\log(K) \sim \mathcal{N}(0, 1)$), with an exponential covariance (correlation structure). The domain is $D = [0, 1]$ and the boundary conditions are $p(0) = 1$ and $p(1) = 0$. The dimensionless correlation length of $K(x)$ (l_Y) is equal to 0.2. In order to ensure that the conductivity is differentiable, we use the Karhunen-Loeve (KL) expansion [6] to construct the field. The code available at [7] was used for generating the KL expansion. The eigenfunctions were found numerically to resolve 99% of the energy of the field. Figure 2 shows the first five eigenfunctions and their derivatives. We assume that the KL expansion provides a good model for the conductivity field. Since all of the eigenfunctions are smooth their derivatives can be easily calculated. Here, the derivatives of the eigenfunctions are estimated numerically (by finite differences). Figure 3 shows one realization generated from this KL expansion with multiple different resolutions. For resolutions higher than a hundred grid points, the realization of the log-permeability does not change.

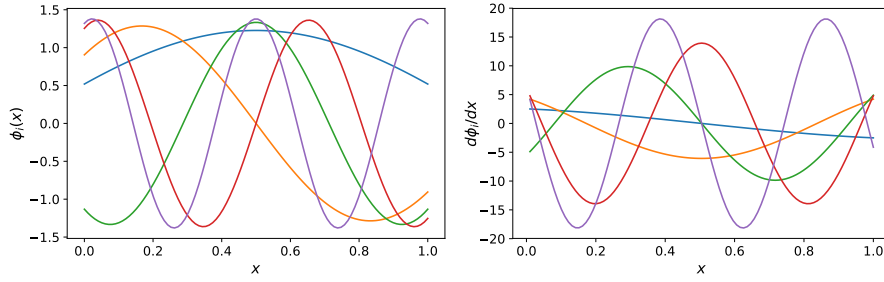


Figure 2: First five eigenfunctions of the covariance function used in example 2 and their derivative.

Figure 4 shows the realization of the permeability field used in this example and its derivative. To ensure that we have resolved the permeability field sufficiently, $K(x)$ was evaluated at $n = 200$ equidistant points. This problem does not have a closed form analytic solution. In this case, the reference solution was found using the finite volume (FV) method [1]. The FV solution was found using the fipy package [8]. The FV solution for all permeability fields shown in Fig. 3 are illustrated in Fig. 5. The solution is converged for $n = 200$ and higher resolutions, hence we will use the FV solution for $n = 200$ as our reference solution. The reference FV solution is compared to its Monte Carlo estimate for selected points in Fig. 6. It can be seen that the stochastic method provides very accurate estimates to the FV reference solution. It is also observed that the quality of the MC estimates improve by increasing the number of trials.

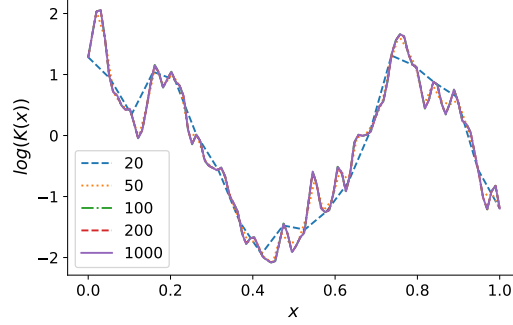


Figure 3: One realization of the logarithm of the permeability field described in example 2, evaluated with five different resolutions.

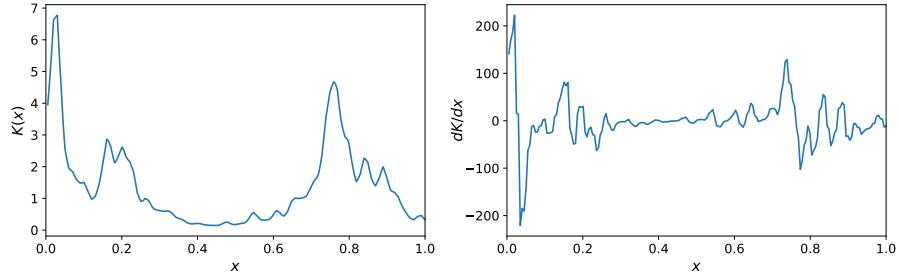


Figure 4: One realization of the permeability field described in example 2 along with its derivative. The derivative is used as the drift term in the stochastic counterpart of the elliptic problem.

4. Illustrative examples for uncertainty quantification

In this section we use backward walks on boundary using the stochastic counterpart of the conservation operator, \mathcal{L}_1 , to quantify the uncertainty in the solution of elliptic PDEs with a random heterogeneous conductivity field. In order to estimate the uncertainty in the solution, $p(x)$, one thousand realizations of a log-normal conductivity field with zero mean and a variance of one were considered. In this example, the conductivity field has a Gaussian correlation structure with $l_Y = 0.2$. The domain and boundary conditions are identical to example 1. Realizations of the described Gaussian conductivity field were generated and the flow equation was solved using the finite volume method for all of these realizations. Figure 7 illustrates a number of these realizations and their corresponding pressure solution.

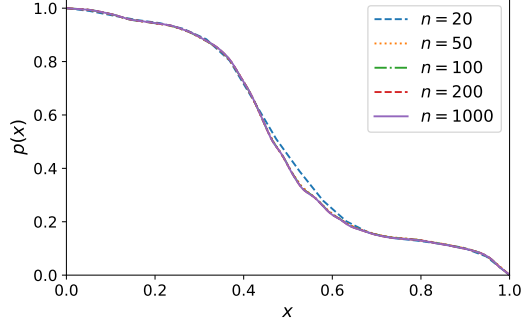


Figure 5: The finite volume solution for the problem described in example 2 with different resolutions.

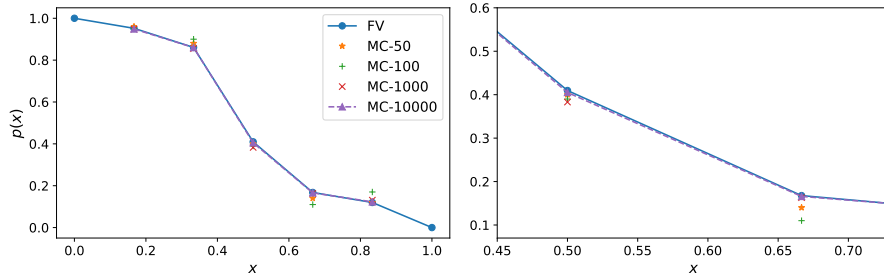


Figure 6: Comparison of the reference FV solution with the MC estimates for example 2 for different number of trials with $dt = 1e-5$.

4.1. Estimating the one-point distribution

The one-point distribution of $p(x)$ at $x = 0.25, 0.5$, and 0.75 , obtained from the proposed stochastic algorithm is compared with reference FV solutions in Fig. 8. The stochastic method provides a good approximation of the pressure distribution at all three locations. It should be noted that the MC estimate of the solution was obtained only for the points of interest without the need for a grid, storing the coefficient matrix of a linear system, or solving a linear system. On the other hand, the FV solution requires a grid and is obtained at all locations on the grid by solving a linear system. In a large domain with uncertain conductivity fields, an optimized implementation of the proposed MC method can be much more efficient than solving a linear system for every realization.

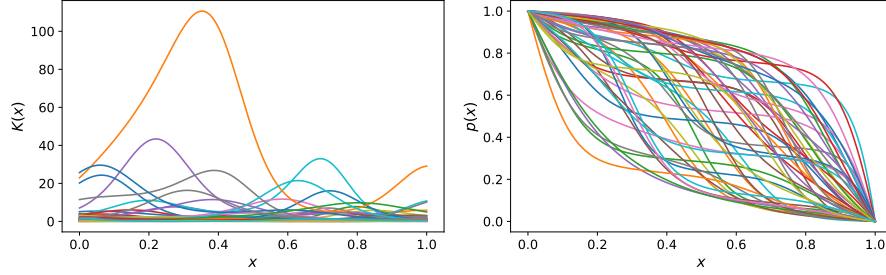


Figure 7: Fifty conductivity realizations generated from the distribution described in example 2 and their corresponding FV pressure solution.

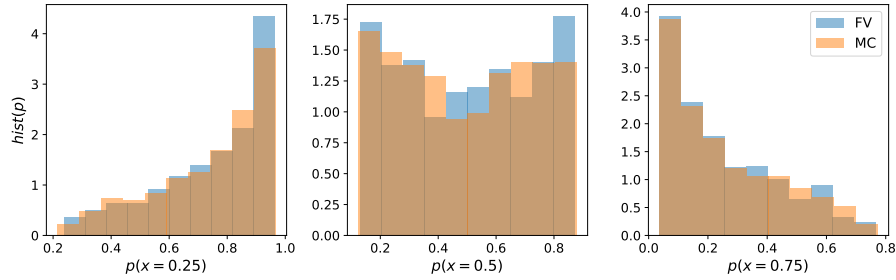


Figure 8: Comparison of the one point histogram of pressure generated from the stochastic solution with $dt = 0.0001$ and 2000 trials for each point and the reference FV solution.

4.2. Estimation of moments

The proposed stochastic method can also be used for estimating the moments of the solution at a given point. Consider estimating the mean solution. Since the MC method provides an unbiased estimate of the solution in each realization, and calculating the mean involves averaging the solution of different realizations, one would expect that random fluctuations around the mean pressure, \bar{p} , in different realizations would cancel out. This suggests that compared to calculating the exact solution for one realization, we could use a significantly smaller number of trials for estimating the mean.

As an example, consider the mean pressure, $\overline{p(x)}$, of the Gaussian conductivity field in section 4.1. Here we estimate $\overline{p(x)}$ at $x = 0.25, 0.5, 0.75$ using the stochastic counterpart of the elliptic problem and compare the results to the mean obtained from the FV simulations. The MC estimate was obtained in 30 experiments each consisting of 1000 realizations of $K(x)$. In each realization, for every point of interest, only one random walk was tracked until hitting the boundary (compared to 10000 for the best solution in example 1). Figure 9

summarizes the result of these experiments. The FV mean is well within the error bars of the MC estimate despite the fact that we only use one random walk in each realization. This result illustrates the potential of the proposed method for significantly reducing the computational cost of obtaining the mean solution.

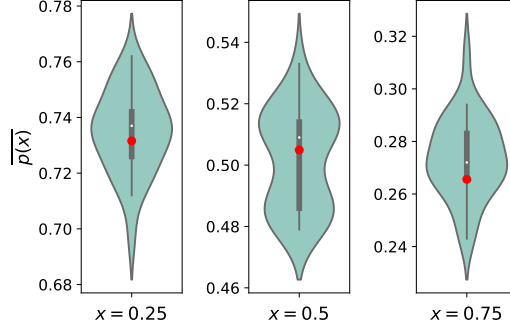


Figure 9: Violin plots of the MC estimate of the mean solution obtained at three point in the domain with one trial per point of interest per realization. The mean from FV simulations is shown by red circles.

The standard deviation, s , of the solution (or any higher moment) can also be estimated using random walks. Figure 10 shows the estimated standard deviation of $p(x)$ at $x = 0.25$, 0.5 , and 0.75 . Similar to the mean, the MC estimate of s was obtained in 30 experiments each involving 1000 realizations of the random field. In each realization of K , at every point where s is estimated, 100 random walks were launched and tracked until hitting the boundary. It can be observed that the standard deviation obtained from the FV solutions is within the distribution of its MC estimates. Compared to the first moment, more trials per realization are needed to obtain a good estimate of s . Since the variance of the solution due to the number of random walks decreases by increasing the number of trials, the quality of the estimated s would improve as the number of trials increase.

5. Conclusions and future work

In this paper, we described the stochastic counterpart of the differential operator in elliptic and parabolic conservation equations with heterogeneous conductivity fields. The stochastic counterpart of these conservation laws allow us to extend backward walks and random walks on boundary, and to use these Monte Carlo methods for solving conservation laws with heterogeneous conductivities. The drift and diffusion functions used in the proposed stochastic representation of the differential operator are obtained from the heterogeneous conductivity field. Several one-dimensional examples show that this method is

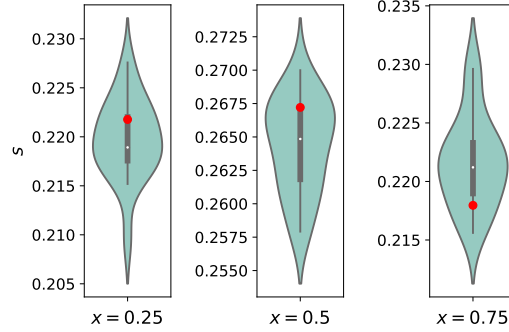


Figure 10: Violin plots of the MC estimate of the standard deviation of the solution obtained at three point in the domain with 100 trials per point of interest per realization. The reference standard deviation from FV simulations is shown by red circles.

capable of accurately obtaining the solution of a deterministic PDE. Moreover, the proposed method was used to calculate accurate estimates of the one point distribution of the solution. Finally, it was shown that the proposed stochastic method can provide a very efficient alternative for estimating the moments of the solution of a random PDE at specific points of interest in the domain.

The proposed stochastic simulations can be accelerated using numerical methods designed for the simulation of diffusion processes. Variance reduction strategies such as antithetics and control variate schemes can be used to decrease the required number of MC trials for a given precision and will be the subject of future investigations. Moreover, the known statistics of the conductivity field can be used to accelerate path generation for random walk simulations. In two and three-dimensional examples that will be the subject of future work, these accelerations can play a key role. In these higher dimensional domains, extra attention should be given to the simulation of the random paths close to the boundary (e.g. obtaining accurate estimate of the exit location). Furthermore, since the random walks only experience the random field locally, generation of complete realizations of the random field can be avoided. In subsurface flow simulations, this could lead to significant computational cost savings in generating geostatistical models for uncertainty quantification. Finally, an effective implementation strategy to increase the efficiency of the algorithm is to partition the particle paths and have dedicated cores that simulate paths in each partition. This implementation strategy will be explored in future investigations.

Acknowledgements

Amir H. Delgosaie is grateful to Daniel M. Tartakovsky and Joseph Bakarji from the Energy Resources Engineering department at Stanford University for

several helpful discussions. Funding for this project was provided by the Stanford University Reservoir Simulation Industrial Affiliates (SUPRI-B) program.

References

References

- [1] H. Versteeg, W. Malalasekera, The finite volume method (1995).
- [2] L. N. Trefethen, D. Bau III, Numerical linear algebra, volume 50, Siam, 1997.
- [3] B. Øksendal, in: Stochastic differential equations, Springer, 2003, pp. 65–84.
- [4] A. J. Chorin, O. H. Hald, Stochastic tools in mathematics and science, volume 3, Springer, 2009.
- [5] K. K. Sabelfeld, N. A. Simonov, Random walks on boundary for solving PDEs, Walter de Gruyter, 1994.
- [6] J. W. Woods, H. Stark, Probability, random processes, and estimation theory for engineers, Prentice-hall, 2000.
- [7] I. Bionis, Introduction to uncertainty quantification, <https://github.com/PredictiveScienceLab/uq-course>, 2018. Accessed: 03/20/2018.
- [8] J. E. Guyer, D. Wheeler, J. A. Warren, Computing in Science and Engineering 11 (2009) 6–15. URL: <http://www.ctcms.nist.gov/fipy>. doi:10.1109/MCSE.2009.52.